Simulation and Design of a Tunable Patch Antenna

Benjamin D. Horwath and Talal Al-Attar

Department of Electrical Engineering, Center for Analog Design and Research
Santa Clara University, Santa Clara, CA 95053-0569, USA
bhorwath@scu.edu, talattar@scu.edu

Abstract **–** A method for designing a tunable microstrip patch antenna is presented, suggesting cooperation between a theoretical transmission line model and a professional electromagnetic simulation tool. Tunable impedance elements are used to perturb the microstrip patch to alter the tuning range of the antenna. Results show excellent correlation between theoretical calculations and simulation data from Sonnet. Finally, guidelines for designing an antenna to be excited by an IMPATT diode are discussed.

Index Terms **–** Tunable Antenna, IMPATT Diode, Sonnet, Microstrip, Patch Antenna

I. INTRODUCTION

Tunable antennas offer several intriguing properties for wireless communications [1-5], ranging from cost savings by combining several analog components into one to introducing new uses, such as an adaptive element for smart antenna systems. The ideal element would offer dynamic control of a significant tuning range of resonance frequencies and bandwidths on a single antenna. To date, attempts to design a truly tunable antenna have been rudimentary, attaining a piece of the goal, such as a shift in resonance frequency at the cost of bandwidth, or vice versa. Some focus is needed to determine the type of excitation that offers total control over the electrical properties of an antenna.

Previously, a theoretical method was explored for tuning microstrip patch antennas by way of a dynamic "black box" impedance element: an ideal component with an unlimited set of values for both resistance and reactance [6]. Such an idealistic approach helped find the bounds of tunability with respect to the antenna's field pattern and identify the most useful implementations of tunable antenna elements. Subsequently, the transmission line model previously used has been improved to include the impact of feedline width and mutual effects, which in turn allows for more accurate design simulations.

The transmission line model offers enough accuracy to quickly optimize not only the antenna dimensions, but also to search for tuning features such as complex impedance values and diode locations to meet design specifications. While more rigorous optimization techniques are available, (such as demonstrated for patch antenna sensitivity analysis with a method of moments [7]) these tools focus specifically on evaluating changes to the physical structure of the antenna only. Significant effort would be needed to modify this technique to include perturbations from an active tunable impedance device, as modeled in this presented research.

As a check against this work, a professional software tool, Sonnet, was used to evaluate the antenna baseline and tuning results derived from the theoretical model. Sonnet uses a method of moments [8] to analyze the electromagnetic properties from the physical dimensions of a circuit. By using Sonnet for this comparison, the previous work can be confirmed with a different computer-aided design methodology. It was found that the two design tools offered complementary benefits, so a natural conclusion was to create a cooperative procedure for designing tunable antennas. This new procedure takes advantage of the optimization flexibility of the theoretical model and the analytical rigor from the easy-to-use Sonnet package.

While the basis of the work was an ideal impedance "black box", the IMPact Avalanche

Submitted On: June 27, 2011
Accepted On: February 9, 2012

Transit Time (IMPATT) diode [9-11] has shown significant promise as a real-world means for achieving tunable antennas. Sonnet design and simulation considerations for integrating an IMPATT diode with a microstrip patch antenna are also discussed.

II. THEORY

The cornerstone of the tunable antenna model is the classic Pues and Van de Capelle [12-14] transmission line model for microstrip antennas. This method uses the dimensions as well as four imaginary radiating slots to represent the radiation properties of the antenna, and is well-known for being simple yet accurate. The model allows one to visualize the antenna as a network of elements as seen in Fig. 1.

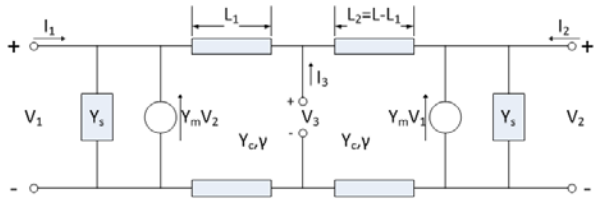

Fig. 1. Three-port network diagram for Pues transmission line model.

Procedurally, the Pues model computes effective parameters for line width W_e, length L_e, dielectric constant ε_{eff}, and loss tangent δ_e that have been adjusted to compensate for the total dimensions of the strip, the strip thickness, and dispersion at the operating frequency. These parameters are then used to find the appropriate characteristic admittance Y_c, propagation constant γ, self-admittance Y_s of the equivalent radiating slot, and mutual admittance effects Y_m. They combine via:

$$Y_{in} = \frac{Y_c^2 + Y_s^2 - Y_m^2 + 2Y_sY_c\coth(\gamma L) - 2Y_mY_c\,\mathrm{csch}(\gamma L)}{Y_s + Y_c\coth(\gamma L)}, \quad (1)$$

to yield an input admittance for the designed antenna at a microstrip feedline located at one edge of the patch.

The relationship in (1) leads directly to the input impedance of the patch antenna, but can be somewhat simplified by use of the transmission line admittance transfer function [5]:

$$Y_i = Y_c\frac{Y_c + Y_l\coth(\gamma L)}{Y_l + Y_c\coth(\gamma L)}, \quad (2)$$

where Y_c is still the characteristic admittance, Y_l is a load admittance at a distance L from an intermediate location, and Y_i is the transferred admittance at that intermediate point. If Y_l is set as the sum of Y_m and Y_s, (2) can be used to find a Y_i at the input edge that has been transferred from the slot and mutual effects of the far edge of the antenna. Then slot and mutual admittances from the input edge can be added to yield the expected input admittance.

In regards to tunability, the transfer function in (2) can be exploited to introduce a tunable element along the length of the patch, connecting the radiating slots of the antenna. For instance, consider some Y_d that represents the admittance of a tunable diode placed at distance L/2 from the patch input. This becomes a new intermediate point, and the transfer function needs to be used twice. First, the far edge admittance, $Y_{l,far}$, is "rolled" a distance L/2 with (2). This creates a $Y_{i,diode}$ that can be added with Y_d (a shunt device) to give a $Y_{l,diode}$. Then, (2) is used again to "roll" the remaining L/2 to the near edge, where it is added with the near edge admittance $Y_{l,input}$ to give a new Y_{in} for the tuned antenna.

This effort suggests another factor impacting antenna tunability: the location of the "black box" on the patch at design time. The addition of another parameter to the design considerations evolves the simple L and W search of the standard patch antenna design procedure to a new process requiring an optimization routine that takes into account not only the antenna dimensions, but Y_d and its location as well.

Generally speaking, the tunable impedance element (or admittance based on preference) provides a perturbation that, in turn, modifies the input impedance to the patch. With the relationship between input impedance and patch dimensions {in light of the documented Pues model and (2)}, this tuned antenna system behaves like a static antenna but with a new W and L at the operating frequency. It is as if the tunable "black box" impedance can electrically stretch or squeeze the patch antenna.

For the tunable microstrip patch antenna designer, the following process is recommended:

i. *Design a basic microstrip patch antenna to establish a baseline for the design using (1)*
ii. *Set design goal(s) for the complete tunable antenna system, such as frequency operating range or a desired Z_{in}*
iii. *Begin iterative loop to step through different locations and tuning values for the tunable impedance (admittance) element*

iv. Use (2) to find the transferred shunt admittance of the radiating slot plus mutual effects at the location of the "black box"
v. Combine the tunable and transferred admittances; use (2) to transfer to the input
vi. Combine the new transferred admittance with the near radiating slot and mutual effects to get the new input admittance
vii. Repeat the design process in reverse if the 'tuned' width and length are desired
viii. Compare to design goal(s) and continue iterations until desired effects are achieved

This procedure can be used to evaluate the impact of the tuned impedance values from the "black box" at several different locations on the baseline antenna. Checking this work against an accepted software tool is vital to ensuring its reliability. Comparison with results from Sonnet is presented below.

III. RESULTS

As a baseline, a microstrip patch antenna is designed with a resonance frequency at f_o = 2.4 GHz. The dimensions of the patch are W = 2.42259 cm and L = 4.15922 cm with strip thickness t = 35 μm on a substrate having ε_r = 2.2 and height h = 0.15875 cm. These substrate parameters mimic Rogers RT/duroid 5880, a well-known, commercially available copper substrate. The feedline is matched to 50 Ω at 2.4 GHz with a width of 0.484517 cm. Fig. 2 illustrates the antenna layout with a "black box" at the input.

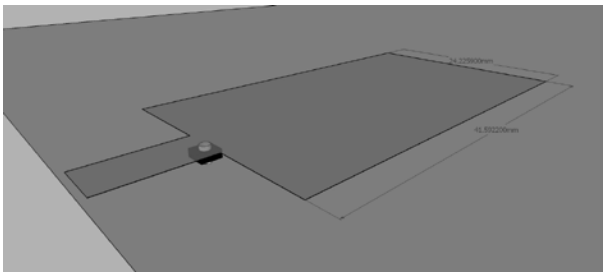

Fig. 2. Physical layout of microstrip patch antenna with black box element at the input.

Using the implemented model based on Pues [12-14], the baseline antenna is calculated to have Z_{in} = 979.58 Ω, Z_c = 14.3269 Ω, Z_s = 15.432 - j185.92 Ω, Z_m = 1150.1 + j4130.6 Ω, and γ = 0.0326 + j72.3651. Sonnet simulated this antenna to resonate slightly higher at 2.404 GHz with Z_{in} = 979.9 Ω. The nearly identical Z_{in} responses for the theoretical model and Sonnet are plotted in Fig. 3.

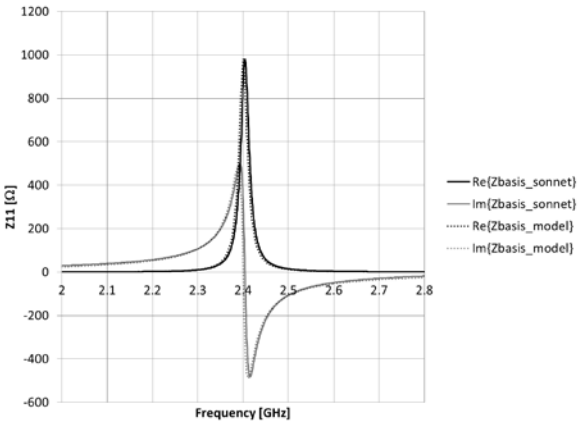

Fig. 3. Comparison of input impedance vs. frequency for designed patch antenna from the theoretical model and equivalent in Sonnet.

To evaluate the impact of placing the tuning element at various locations along the midline of the patch antenna, the Sonnet geometry for the patch was modified to include a via port at the desired locations. It is at this port the "black box" will be added in shunt to perturb the antenna. The first step was to choose a cell size for Sonnet since it is desirable to make the via as small as possible to reduce parasitic capacitance, yet shrinking the cell multiplies the memory requirement for Sonnet's calculations. For a single cell implementation, the final dimensions of the via were 202.889 μm long by 230.723 μm wide by 158.75 μm deep (10% of the dielectric height).

A new geometry was created to include the via port along the midline at one-tenth increments of the patch length from the feedline input to the far edge of the antenna. The net parasitic capacitance is seemingly significant, shifting the resonance frequency of the new geometries lower by about 10-15 MHz, yet the field patterns are comparable at 2.4 GHz, as shown in Figs. 4a and b. By comparing the Z_{in} responses for the basis and via-port geometries, it was determined the shunt capacitance introduced averages about 64 fF around the 2.4 GHz operating range.

Analyzing the impact of the tuning elements was carried out by stepping through values within a desired impedance range for the "black box" and one-tenth increments of the antenna length. It is

assumed that the tunable "black box" has two extremes: 1) positive resistance with inductance (extreme value of 30 + j190 Ω), 2) negative resistance with capacitance (extreme value of -5 - j100 Ω). The tuning range bounds were chosen to provide a bit of reality to this theoretical search, as it is hoped to replicate these results in the lab. Thus, the values were picked to emulate measurement results from previous IMPATT diode work [9-11], and also result in a good degree of tunability for the proposed antenna system.

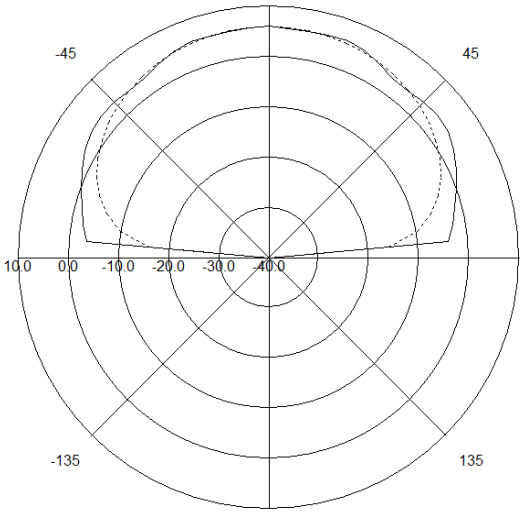

Fig. 4a. Field pattern for basis antenna. Solid line: E-plane, Dashed line: H-plane.

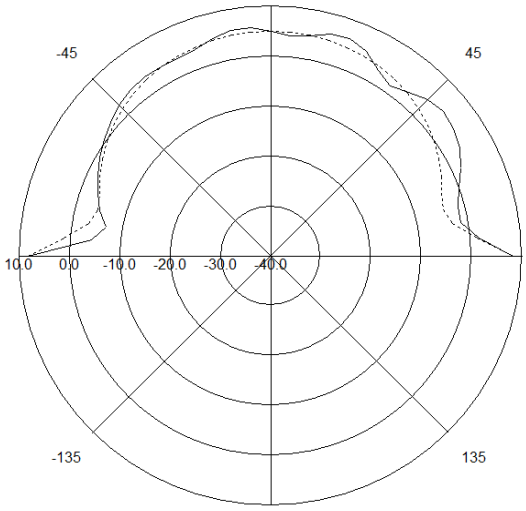

Fig. 4b. Field pattern for antenna with via @ 0.2L. Solid line: E-plane, Dashed line: H-plane.

Using the procedure given in Section II for an element tuned to -5 - j100 Ω and placed at the input to the patch, the resultant Z_{in} is calculated and plotted in Fig. 5, highlighting a downward resonance frequency shift of 107 MHz to 2.293 GHz. Correspondingly, the Sonnet Netlist function is used to combine the antenna with a .z1p data file and plot the results in Figs. 6 and 7.

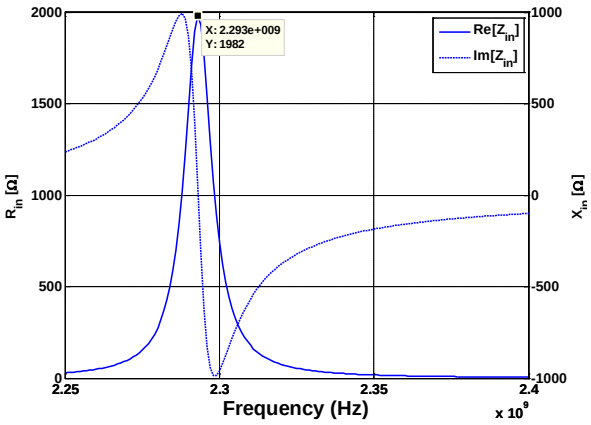

Fig. 5. Input impedance versus frequency for patch antenna tuned with Z_d = -5-j100Ω from theoretical model with resonance frequency at 2.293 GHz.

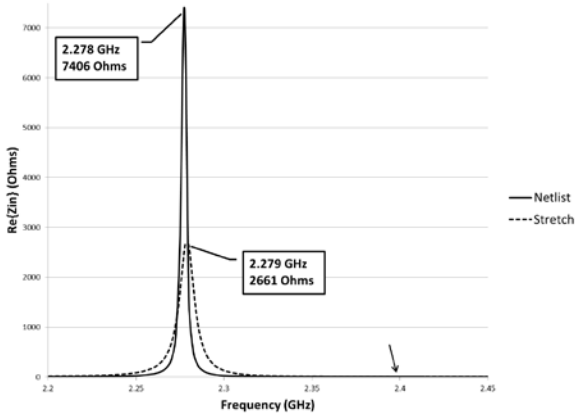

Fig. 6. Input resistance vs. frequency for tuned antenna (Z_d=-5-j100Ω) in Sonnet: networked components vs. stretched dimensions. Arrow indicates match at frequency of 2.4 GHz.

Additionally, Figs. 6 and 7 display a "stretched" antenna based on the tuned input impedance at 2.4 GHz (labeled 'stretch'). For this scenario, the equivalent patch dimensions are a 7.4% longer length of 4.46902 cm and a 28.2% shorter width of 1.74059 cm, demonstrating the ability to tune beyond the physical area of the

antenna. The Netlist and "stretched" curves differ, with comparable resonance frequencies at 2.278 and 2.279 GHz, respectively, but have a significant discrepancy in input impedance. It should also be noted that the Netlist curve included the additional capacitance from the via port, while the 'stretched' analysis does not.

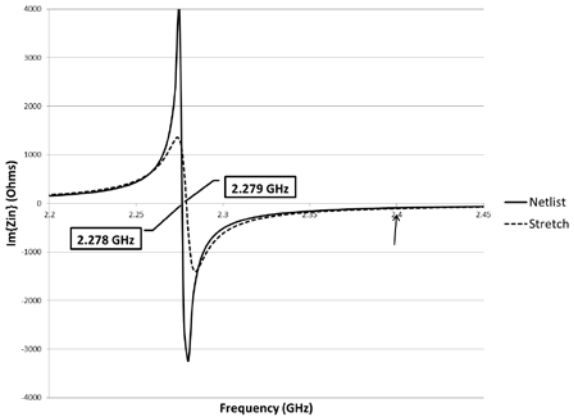

Fig. 7. Input reactance vs. frequency for tuned antenna (Z_d=-5-j100Ω) in Sonnet: networked components vs. stretched dimensions. Arrow indicates match at frequency of 2.4 GHz.

The difference between the Netlist and "stretched" input impedance results highlights an initial flaw in the proposed analysis procedure: there is an important distinction between the operating range and the designed resonance frequency. Subsequent research will focus on the equivalent "tuned" dimensions over an entire desired operating range, and reporting how well that range is met for the "new" length and width.

To summarize the comparison, results from the two extreme tuning scenarios, -5-j100Ω and 30+j190Ω, at each of the predetermined locations are captured in Table 1 to assess the impact to moving the tuning element along the midline of the patch antenna. The first observation to be made is to note that adding -5-j100Ω anywhere causes the resonance frequency to shift towards DC, while 30+j190Ω moves f_{res} higher. Next, the shift seen due to the inclusion of the via port in the Sonnet geometries was consistent through all results: not only in the difference of the 2 tuning scenarios, but also as the delta between the model and Sonnet. There is an excellent correlation between the results of the model and those of Sonnet, validating the use of the model as a design guide for placing tunable elements.

Table 1: Impact of tuning at several locations – no load (nl), -5-j100Ω (nrc), and 30+j190Ω (prl)

		Model/Sonnet
Case	**f_{res} (GHz)**	**Z11 (Ω)**
Basis	2.4/2.404	979.6/979.9
0.0L, nl	2.4/2.394	979.6/1102
0.0L, nrc	2.293/2.278	1982/7406
0.0L, prl	2.456/2.445	541/505
0.4L, nl	2.4/2.392	979.6/969.8
0.4L, nrc	2.39/2.381	982.4/958.6
0.4L, prl	2.405/2.397	932/933.2
0.6L, nl	2.4/2.391	979.6/1023
0.6L, nrc	2.391/2.381	1068/1148
0.6L, prl	2.405/2.395	896.2/935.1
1.0L, nl	2.4/2.394	979.6/971.5
1.0L, nrc	2.294/2.273	2046/2843
1.0L, prl	2.456/2.448	538.8/553.0

A third observation can be seen from Table 1 that the closer the location is to 0.5L, the lesser the impact to the f_{res} shift. There may be other benefits to placing the tuning element at these inner locations such as dynamic input impedance tuning, but this was not evaluated during the analysis. For this work, the input feedline meets the patch at the very edge (as seen in Fig. 2 and not indented), creating an impedance mismatch. The input may be notched further inside to provide a better Z match in subsequent work.

The final observation is that there is symmetry about the 0.5L point, as can be seen by comparing the results between 0.0L and 1.0L as well as 0.4L and 0.6L in Table 1. Each case offers very similar results whether it is on the near or far side of the midpoint, and analysis of the impedance response in the surrounding spectrum confirms comparable results. In a way, this makes the choice of tuning location a bit easier, since the impact on one side mirrors the other side. In turn, this may offer more degrees of freedom to choose locations that bring other benefits such as system layout convenience.

The largest discrepancies in the results can be seen in the magnitude of Z_{in} at resonance. Of strongest note is the difference in Z_{in} at the 0.0L location for the -5-j100Ω scenario. Much of the disparity can be linked to the resolution of the calculations, as the input impedance behaves

asymptotically near resonance.

As a final remark, the work presented intuitively leads to a design procedure that leverages the advantages of the two models. The designer can begin constructing the dimensions of the desired antenna and tuning characteristics with an optimization tool like the theoretical transmission line model presented. Once a framework is determined, Sonnet's advanced layout and simulation features can be used to verify performance and establish a design feedback loop with physical data such as area and boundaries. Such a complementary effort between the two tools could be integrated via SonnetLab, which offers a link between MATLAB and Sonnet for automating their interaction.

IV. IMPATT DIODES

Several methods for tuning antenna elements have been proposed over the years, most notably the usage of varactors and/or specially-biased FETs [15]. These are often limited to just resistance or capacitance and tend to fall short for improving antenna robustness.

The tuning range chosen for this investigation is based on values that have been achieved with the IMPATT diode [9-11], a promising method for achieving a range of impedance values through a single device. A DC bias, which should be well isolated from the RF signal, controls the avalanche frequency, and, hence, the diode impedance. Fig. 8 shows the model for the IMPATT diode before and after the avalanche frequency.

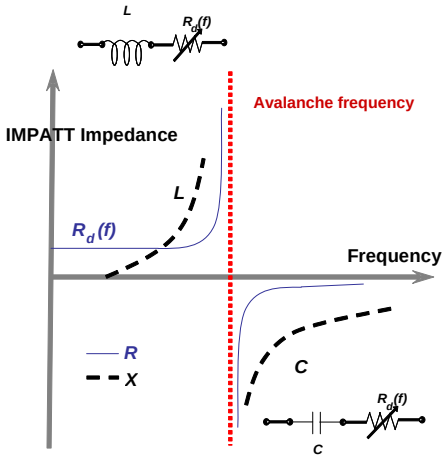

Fig. 8. Model for IMPATT impedance vs. frequency, for both sides of avalanche frequency.

The impedance capabilities of the IMPATT diode range from $R + j\omega L$ to $-R + 1/j\omega C$, as modeled with the "black box". The necessary tuning range can be achieved by careful design of the diode dimensions. This means that when combined with a patch antenna, the properties can be tuned solely by the biasing of the IMPATT diode. Using the model to find ideal locations for IMPATT diodes along the patch, designers could quickly layout and analyze a tunable antenna with co-located IMPATT diodes in Sonnet.

V. CONCLUSIONS AND REMARKS

In summary, the work presented demonstrates a good marriage between results from the transmission line model and Sonnet. This relationship naturally leads to a collaborative design procedure for tunable patch antennas. To further advance the study of exciting a microstrip patch with impedance elements, Sonnet could improve the means of locating shunt impedances inside a structure (not just at edges) for evaluation. Finally, it should be pointed out that the final step of implementing the proposed tunable antenna with an IMPATT diode is made significantly simpler with the advanced layout and analysis features of the Sonnet tool.

REFERENCES

[1] J. C. Liberti and T.S. Rappaport, *Smart Antennas for Wireless Communications: IS-95 and Third Generation CDMA Applications,* Upper Saddle River, NJ: Prentice Hall PTR, pp. 81-116, 1999.

[2] W. L. Stutzman and G. A. Thiele, *Antenna Theory and Design*, New York, NY: John Wiley & Sons, 1981.

[3] S. J. Orfanidis, *Electromagnetic Waves and Antennas*, Piscataway, NJ: Electrical and Computer Engineering Department, Rutgers University, 2008. http://www.ece.rutgers.edu/~orfanidi/ewa/

[4] C. A. Balanis, *Antenna Theory*, Hoboken, NJ: John Wiley & Sons, pp. 811-843, 2005.

[5] D. K. Cheng, *Field and Wave Electromagnetics*, Reading, MA: Addison-Wesley Publishing Company, 1989.

[6] B. D. Horwath and T. Al-Attar, "Evaluating the Robustness of Tunable Adaptive Antenna Arrays," *IEEE 11th Annual Wireless and Microwave Technology Conference (WAMICON),* pp.1-5, 12-13 April 2010.

[7] Y. Zhang, N. K. Nikolova, and M. H. Bakr, "Input Impedance Sensitivity Analysis of Patch

Antenna with Discrete Perturbations on Method-of-Moment Grids," *Applied Computational Electromagnetics Society (ACES) Journal*, vol. 25, no. 10, pp. 867 – 876, October 2010.

[8] J. C. Rautio and R. F. Harrington, "An Electromagnetic Time-Harmonic Analysis of Shielded Microstrip Circuits," *IEEE Trans. Microwave Theory Tech.*, vol. MTT-35, pp. 726-730, Aug. 1987.

[9] T. Al-Attar and T. H. Lee, "Monolithic Integrated Millimeter-Wave IMPATT Transmitter in Standard CMOS Technology," *IEEE Transactions on Microwave Theory and Techniques*, vol. 53, issue 11, pp. 3557-3561, November 2005.

[10] T. Al-Attar, M.D. Mulligan, and T.H. Lee, "Lateral IMPATT Diodes in Standard CMOS Technology," *IEEE International Electron Devices Meeting*, pp. 459-462, December 13-15, 2004.

[11] T. Al-Attar, "Simulation and Layout of On-Chip Microstrip Patch Antenna in Standard CMOS Technology," *Applied Computational Electromagnetics Society (ACES), 26th Annual Review of Progress in*, pp. 866-871, April 26-29, 2010.

[12] H. Pues and A. van de Capelle, "Accurate transmission-line model for the rectangular microstrip antenna," *Microwaves, Optics and Antennas, IEE Proceedings H*, vol. 131, no. 6, pp. 334-340, December 1984.

[13] E. Hammerstad and O. Jensen, "Accurate Models for Microstrip Computer-Aided Design," *Microwave symposium Digest, 1980 IEEE MTT-S International*, pp. 407-409, 28-30 May 1980.

[14] M. Kirschning, R. H. Jansen, and N.H.L. Koster, "Accurate Model for Open End Effect of Microstrip Lines," *Electronics Letters*, vol. 17, no. 3, pp. 123-125, February 5, 1981.

[15] Libo Huang and P. Russer, "Electrically Tunable Antenna Design Procedure for Mobile Applications," *IEEE Transactions on Microwave Theory and Techniques,* vol. 56, no. 12, pp. 2789-2797, Dec. 2008.

Benjamin D. Horwath is a 2nd year Ph.D. student in the Department of Electrical Engineering at Santa Clara University. Ben has held engineering, marketing, and business development positions with Corning Incorporated, Phaethon Communications, and his own start-up, AirRay Systems. Prior to his doctorate education, Ben obtained his B.Sc. in Chemical Engineering at Penn State University and M.Sc. in Electrical Engineering at Santa Clara University. His primary research is currently focused on smart antenna systems for mobile devices.

Dr. Talal Al-Attar has over 10 years in teaching experience in Electrical Engineering between Kuwait University, Stanford University and Santa Clara University. He received the B.S., M.S. from Kuwait University and his Ph.D degree from Stanford University. His doctoral work focused on IMPATT modeling at millimeter-wave range, on-chip integration of microstrip patch antennas and transmission lines in standard CMOS Technology.

He worked as a senior design and device engineer at Volterra Semiconductor [2004 - 2007], and a senior member of consulting staff at Sabio Labs [2007]. Dr. Al-Attar joined Magma Design Automation in 2008 when it acquired Sabio Labs. He joined SCU in 2006 as an adjunct professor, then lecturer, and finally as a full-time assistant professor.

His primary research interests includes IMPATT Modeling and scaling in Standard CMOS Technology, Analog design optimization, Microstrip Patch Antenna on-chip for 60GHz and 77GHz applications, Data Converters, LDMOS modeling for RF applications, and UWB measurements.

Dr. Al-Attar contributed to two books in CMOS RFIC and Planar Microwave Engineering. He currently serves on the committees of Radio and Wireless Symposium (RWS) as a student paper competition chair, and he is a member of the IEEE and the ASEE.